Impact of bioenergy crops expansion on climate-carbon cycle feedbacks in overshoot scenarios

Irina Melnikova[1,2], Olivier Boucher[1], Patricia Cadule[1], Katsumasa Tanaka[2,3], Thomas Gasser[4], Tomohiro Hajima[5], Yann Quilcaille[6], Hideo Shiogama[3], Roland Séférian[7], Kaoru Tachiiri[3,5], Nicolas Vuichard[2], Tokuta Yokohata[3] and Philippe Ciais[2]

[1]Institut Pierre-Simon Laplace (IPSL), Sorbonne Université / CNRS, Paris, France
[2]Laboratoire des Sciences du Climat et de l'Environnement (LSCE), IPSL, Commissariat à l'énergie atomique et aux énergies alternatives (CEA/ CNRS/ UVSQ), Université Paris-Saclay, Gif-sur-Yvette, France
[3]Earth System Division, National Institute for Environmental Studies (NIES), Tsukuba, Japan
[4]International Institute for Applied Systems Analysis (IIASA), Vienna, Austria
[5]Research Institute for Global Change, Japan Agency for Marine-Earth Science and Technology, Kanazawaku, Japan
[6]IIASA, Vienna, Austria; now at Institute for Atmospheric and Climate Science, ETH Zürich, Switzerland
[7]CNRM, Université de Toulouse, Météo-France, CNRS, Toulouse, France

Correspondence to: Irina Melnikova (imelnikova@lsce.ipsl.fr)

Supplementary material

Table S1: DOI of simulations used by each model in this study

ESM		IPSL-CM6A-LR	CNRM-ESM2-1	CanESM5	MIROC-ES2L	UKESM1-0-LL
piControl	Ensemble members	r1i1p1f1	r1i1p1f2	r1i1p1f1, r1i1p2f1	r1i1p1f2	r1i1p1f2 (parent to r4..)
	DOI	https://doi.org/10.22033/ESGF/CMIP6.5251	https://doi.org/10.22033/ESGF/CMIP6.4165	https://doi.org/10.22033/ESGF/CMIP6.3673	https://doi.org/10.22033/ESGF/CMIP6.5710	https://doi.org/10.22033/ESGF/CMIP6.6298
historical	Ensemble members	r1i1p1f1	r1i1p1f2	r1i1p1f1	r1i1p1f2	r4i1p1f2
	Branching year	1910	1850	5201	1850	1960
	DOI	https://doi.org/10.22033/ESGF/CMIP6.5195	https://doi.org/10.22033/ESGF/CMIP6.4068	https://doi.org/10.22033/ESGF/CMIP6.3610	https://doi.org/10.22033/ESGF/CMIP6.5602	https://doi.org/10.22033/ESGF/CMIP6.6113
hist-noLu (and historical)*	Ensemble members	r1i1p1f1 r2i1p1f1 r3i1p1f1 r4i1p1f1	r1i1p1f2 r2i1p1f2 r3i1p1f2 r4i1p1f2	r1i1p1f1 r2i1p1f1 r3i1p1f1 r4i1p1f1	r1i1p1f2	r1i1p1f2 r2i1p1f2 r3i1p1f2 r4i1p1f2
	DOI (hist-noLu)	http://doi.org/10.22033/ESGF/CMIP6.5189	http://doi.org/10.22033/ESGF/CMIP6.4049	http://doi.org/10.22033/ESGF/CMIP6.3602	http://doi.org/10.22033/ESGF/CMIP6.5584	http://doi.org/10.22033/ESGF/CMIP6.6060
ssp534-over	Ensemble members	r1i1p1f1	r1i1p1f2	r1i1p1f1	r1i1p1f2	r4i1p1f2
	Branching year	2040	2015	2040	2015	2040
	DOI	https://doi.org/10.22033/ESGF/CMIP6.5269	https://doi.org/10.22033/ESGF/CMIP6.4221	https://doi.org/10.22033/ESGF/CMIP6.3694	https://doi.org/10.22033/ESGF/CMIP6.5767	https://doi.org/10.22033/ESGF/CMIP6.6397
ssp585	Ensemble members	r1i1p1f1	r1i1p1f2	r1i1p1f1	r1i1p1f2	r4i1p1f2
	Branching year	2015		2015		2015
	DOI	https://doi.org/10.22033/ESGF/CMIP6.5271		https://doi.org/10.22033/ESGF/CMIP6.3696		https://doi.org/10.22033/ESGF/CMIP6.6405
hist-bgc	Ensemble members	r1i1p1f1	r1i1p1f2	r1i1p2f1	r1i1p1f2	r4i1p1f2
	Branching year	1910	1850	5550	1850	1960
	DOI		https://doi.org/10.22033/ESGF/CMIP6.4047	https://doi.org/10.22033/ESGF/CMIP6.3600	https://doi.org/10.22033/ESGF/CMIP6.5582	https://doi.org/10.22033/ESGF/CMIP6.6055
ssp534-over-bgc	Ensemble members	r1i1p1f1	r1i1p1f2	r1i1p2f1	r1i1p1f2	r4i1p1f2
	Branching year	2040	2015	2040	2015	2040
	DOI		https://doi.org/10.22033/ESGF/CMIP6.4223	https://doi.org/10.22033/ESGF/CMIP6.3695	https://doi.org/10.22033/ESGF/CMIP6.5769	https://doi.org/10.22033/ESGF/CMIP6.6401
ssp585-bgc	Ensemble members	r1i1p1f1	r1i1p1f2	r1i1p2f1	r1i1p1f2	r4i1p1f2
	Branching year	2015		2015		2015
	DOI			https://doi.org/10.22033/ESGF/CMIP6.3697		https://doi.org/10.22033/ESGF/CMIP6.6409

*While one ensemble member of historical simulations is used for the analysis, we use an ensemble mean of all available ensemble members to evaluate the historical LUC emissions.

Table S2: Carbon-concentration β (GtC ppm^{-1}) and carbon-climate γ (GtC $°C^{-1}$) feedback parameters estimated by three approaches and five ESMs, averaged over 2090–2100 under SSP5-3.4-OS pathway.

	IPSL-CM6A-LR	CNRM-ESM2-1	CanESM5	MIROC-ES2L	UKESM1-0-LL
Global β (GtC ppm^{-1})	**1.24**	**3.96**	**1.66**	**1.65**	**1.14**
β LUC (fLuc)	-0.62	-0.69			
β noLUC (fLuc)	1.86	3.87			
β LUC (crop threshold)	0.07	0.55	-0.38	-0.08	0.09
β noLUC (crop threshold)	1.17	2.63	1.21	1.01	1.59
β LUC (two sim-ns since 1850)	-1.23			-0.63	
β noLUC (two sim-ns since 1850)	2.48			2.30	
β LUC (two sim-ns since 2040)	-0.13				
β noLUC (two sim-ns since 2040)	1.37				
Global γ (GtC $°C^{-1}$)	**-18.45**	**-114.30**	**-36.96**	**-99.33**	**-52.32**
γ LUC (fLuc)	0.82	0.64			
γ noLUC (fLuc)	-10.32	-94.32			
γ LUC (crop threshold)	-1.50	-22.08	-4.62	-4.36	-16.67
γ noLUC (crop threshold)	-7.96	-71.63	-11.62	-31.15	-75.99
γ LUC (two sim-ns since 1850)	-5.33			-17.41	
γ noLUC (two sim-ns since 1850)	-13.12			-69.08	
γ LUC (two sim-ns since 2040)	2.22				
γ noLUC (two sim-ns since 2040)	-69.08				

Table S3: Carbon-concentration β (GtC ppm^{-1}) and carbon-climate γ (GtC $°C^{-1}$) feedback parameters mean values estimated by three approaches and five ESMs averaged over 2090–2100 under SSP5-3.4-OS pathway (the values of IPSL-CM6A-LR and CNRM-ESM2-1 by cropland threshold approach, and IPSL-CM6A-LR by two simulations since 2040 approach are excluded).

	Mean	SD	Cumulative contribution over 2000–2100 (GtC)
Global β (GtC ppm^{-1})	1.93	1.16	
β LUC	-0.51	0.44	-42.55 ± 41.08
β noLUC	2.05	0.97	349.56± 129.43
Global γ (GtC $°C^{-1}$)	-64.27	40.99	
γ LUC	-6.70	7.49	-13.00 ± 12.27
γ noLUC	-43.66	35.32	-88.97 ± 76.83

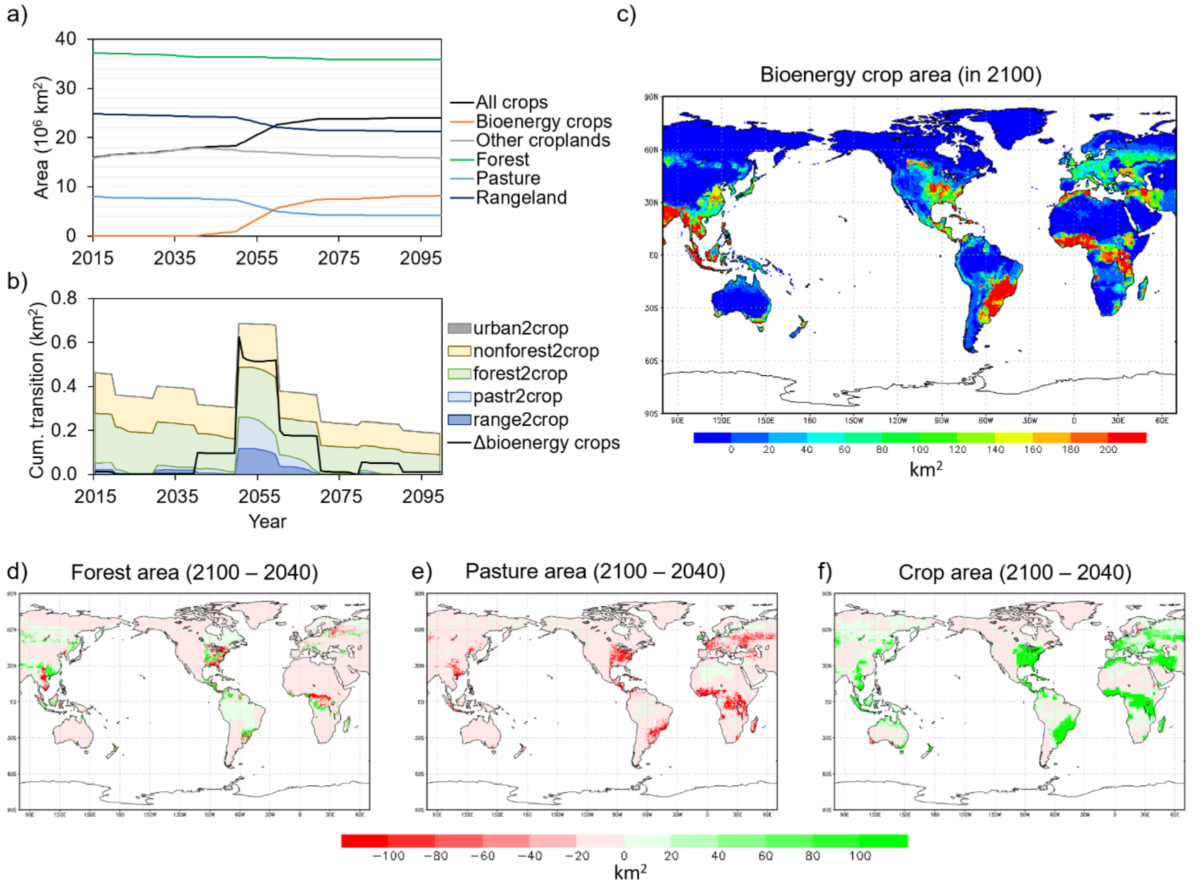

Figure S1: Time series of the changes in the global area of (a) land states, including bioenergy crops, and (b) cumulative transitions, including transitions of rangeland to crop (range2crop), pasture to crop (pastr2crop), primary and secondary forest to crop (forest2crop), primary and secondary non-forest to crop (nonforest2crop), urban area to crop (urban2crop), and yearly change rate of bioenergy crops (Δ bioenergy crops) in 2015-2100 by LUH2. Here the cumulative transitions are given for reference, they are not absolute because they do not include transitions from crops to other states. Panel (c) shows the spatial variation of the bioenergy crops in 2100, (d) the difference in the area of forest, (e) pastures, and (f) croplands in years 2100 and 2040 given by LUH2.

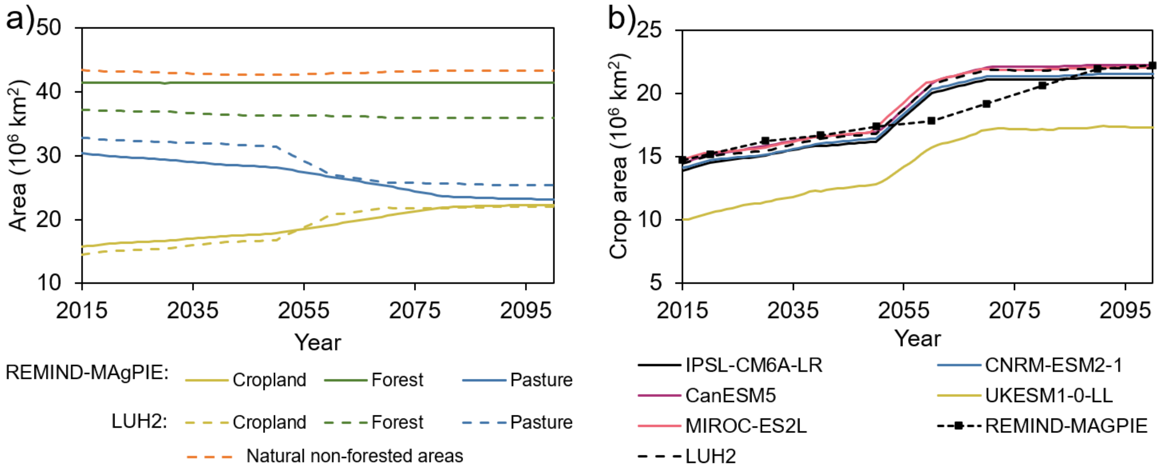

Figure S2: Time series of (a) the changes in the area of croplands, pastures, and forests according to REMIND-MAgPIE (solid lines) and LUH2 (dashed lines) and (b) the area of croplands as prescribed in LUH2 and implemented in REMIND-MAgPIE and five CMIP6 ESMs in 2015–2100 under SSP5-3.4-OS pathway. In panel (a), pastures and rangelands of LUH2 are treated together as pastures; and forest represents the sum of primary forested land and potentially forested secondary land. The croplands of LUH2 include C3, C4 annual crops, C3, C4 perennial crops, and C3 nitrogen-fixing crops. The natural non-forested areas (that include non-forested primary land and potentially non-forested secondary land) of LUH2 are shown for reference.

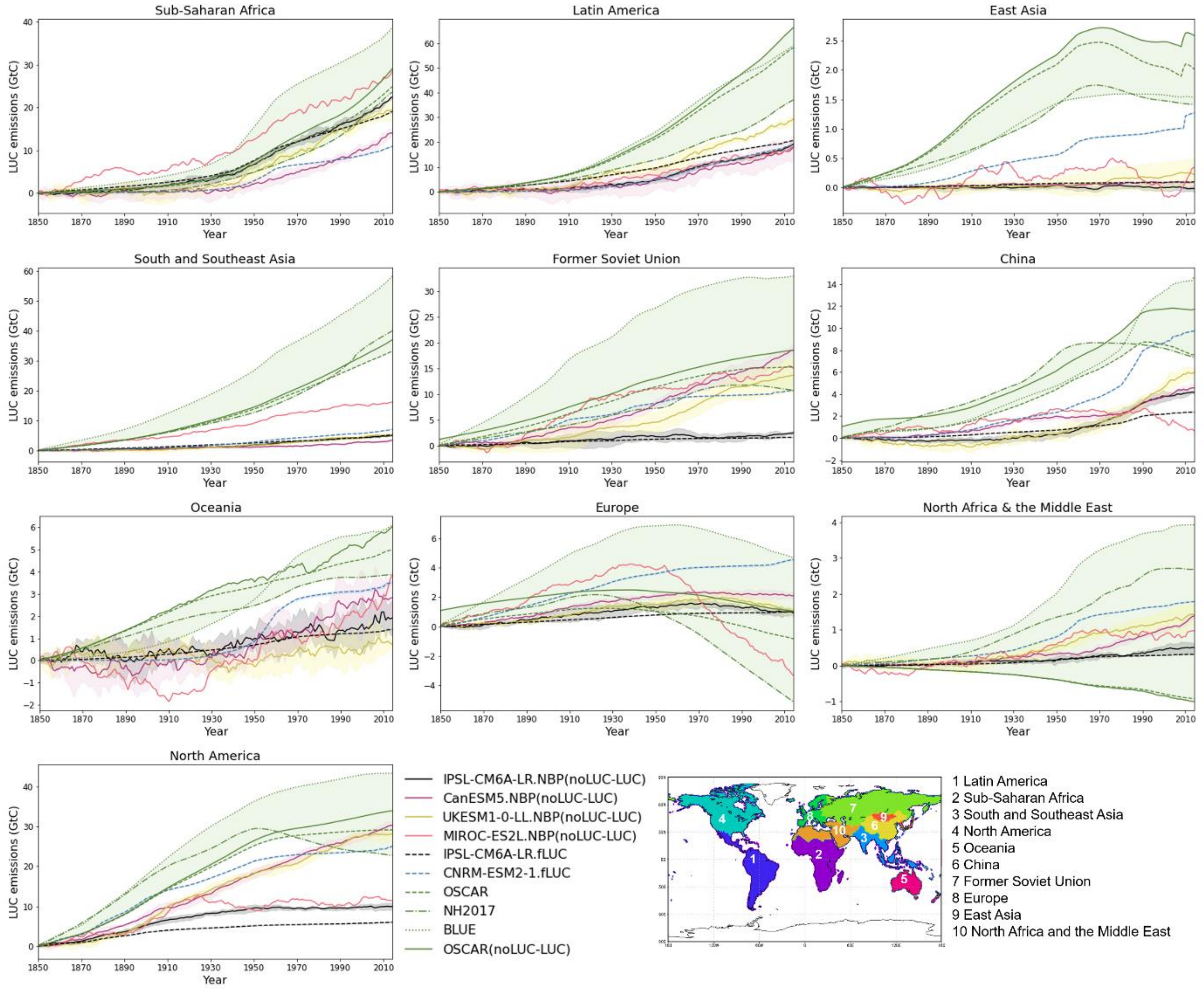

Figure S3: Evaluation of cumulative regional LUC emissions by ESMs against three bookkeeping models. LUC emissions are defined by two methods: 1) the difference in NBP between simulations with and without LUC (solid lines) and 2) the "fLuc" variable provided in CMIP6 (dashed lines). The estimates of the bookkeeping approach using OSCAR are shown for cases with (noLUC-LUC) and without LASC). The range of bookkeeping models is in shaded green.

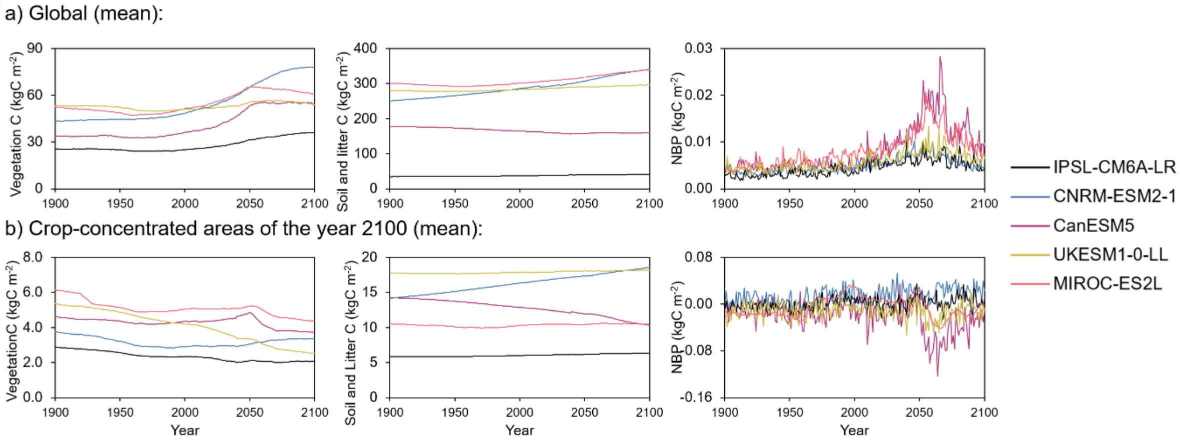

Figure S4: Time series of changes in vegetation and soil, including litter, carbon pools, and NBP (a) globally and (b) in crop-concentrated areas as defined via the "cropland threshold" approach by CMIP6 ESMs. The changes in NBP are given as 10-year moving averages.

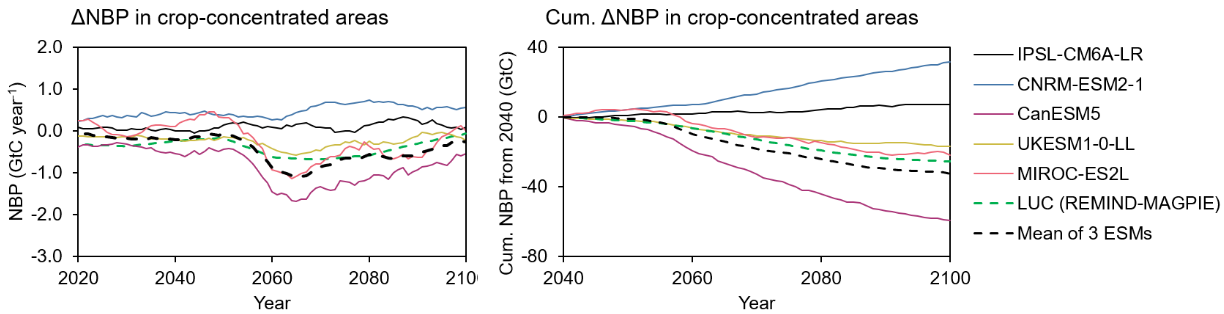

Figure S5: Time series of LUC emissions (left) and cumulative LUC emissions from the year 2040 (right) estimates by CMIP6 ESMs via the "cropland threshold" approach and from REMIND-MAgPIE as given in the IIASA database. ΔNBP refers to the change in NBP in crop-concentrated areas relative to piControl. The mean of three ESMs is calculated using CanESM5, UKESM1-0-LL, and MIROC-ES2L. Positive is sink to the land.

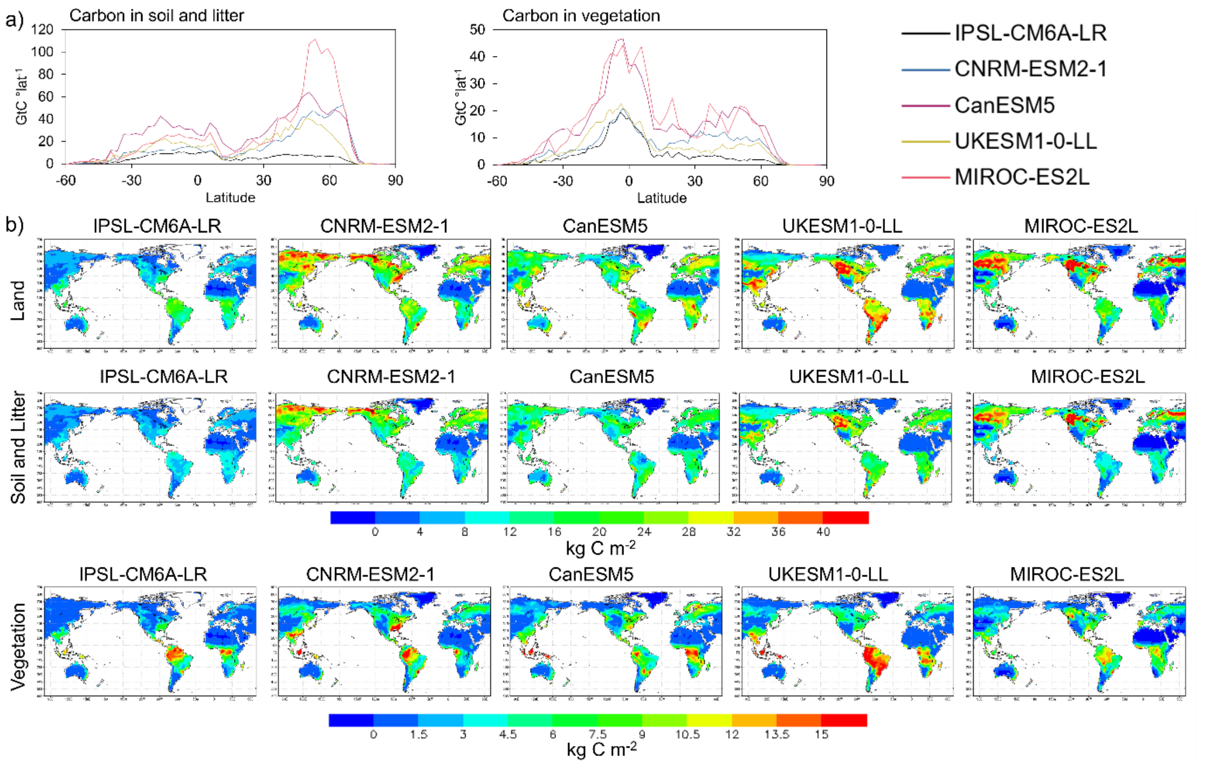

Figure S6: (a) Latitudinal and (b) spatial distributions of the land (soil, including litter, and vegetation) carbon pools in piControl in the five CMIP6 ESMs used in this study.

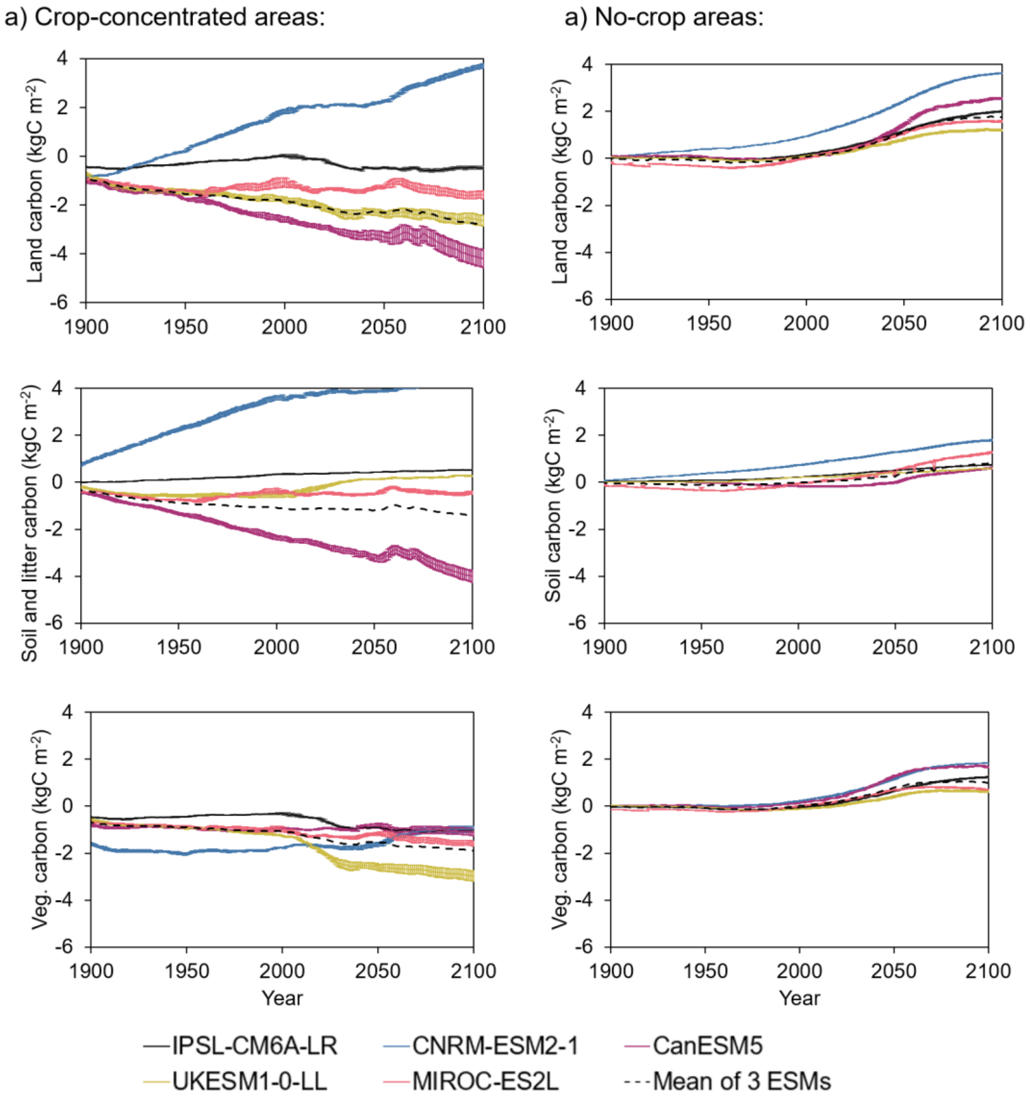

Figure S7: Time series of the spatial mean changes in the land carbon pool and its components, soil, including litter, and vegetation pools, in crop-concentrated and no-crop areas. The mean of three ESMs is calculated using CanESM5, UKESM1-0-LL, and MIROC-ES2L.

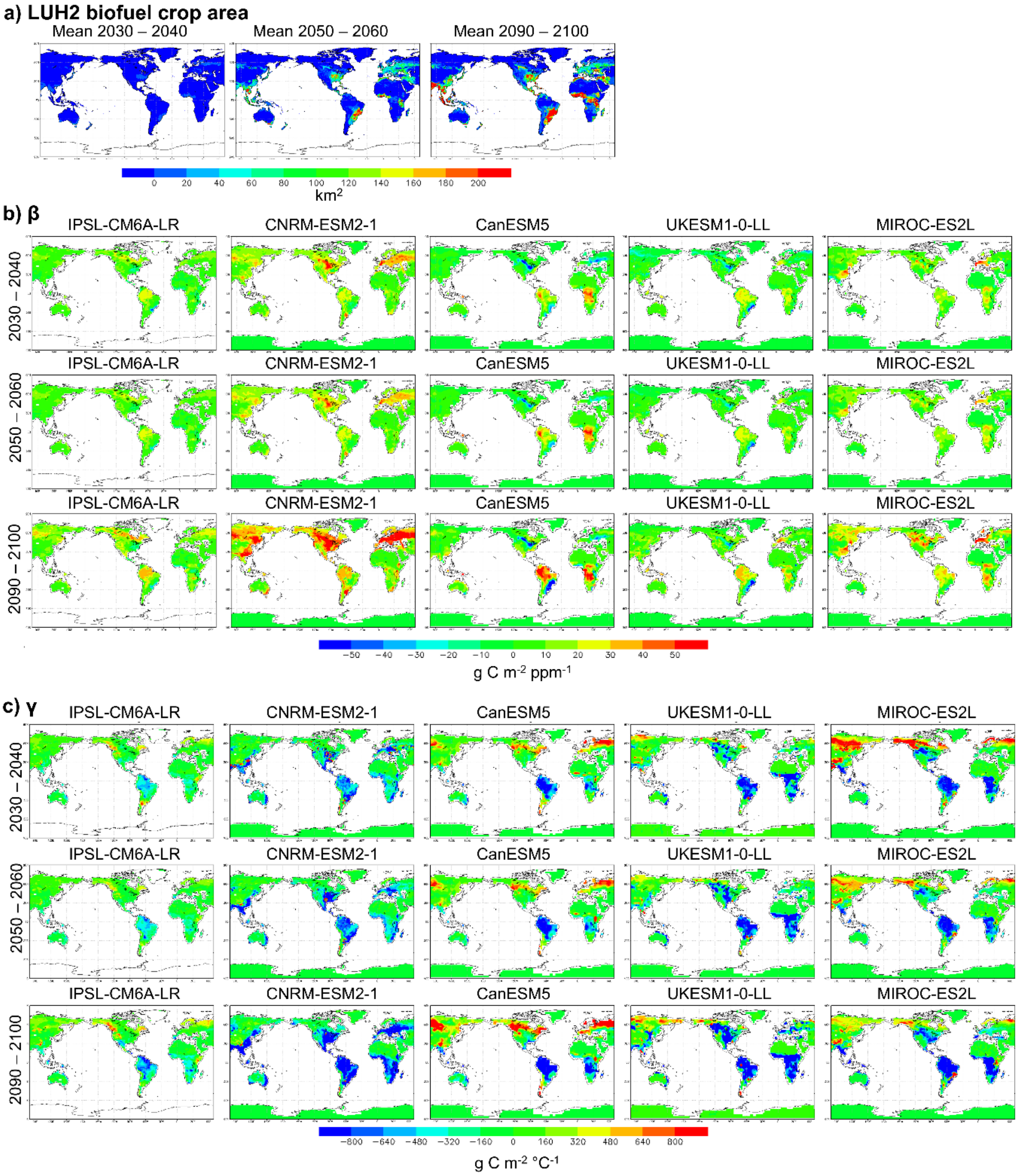

Figure S8: (a) The second-generation biofuel cropland area given in LUH2, the spatial variation of (b) β and (c) γ parameters by five ESMs given as a decadal mean for the 2030s, 2040s, and 2090s.

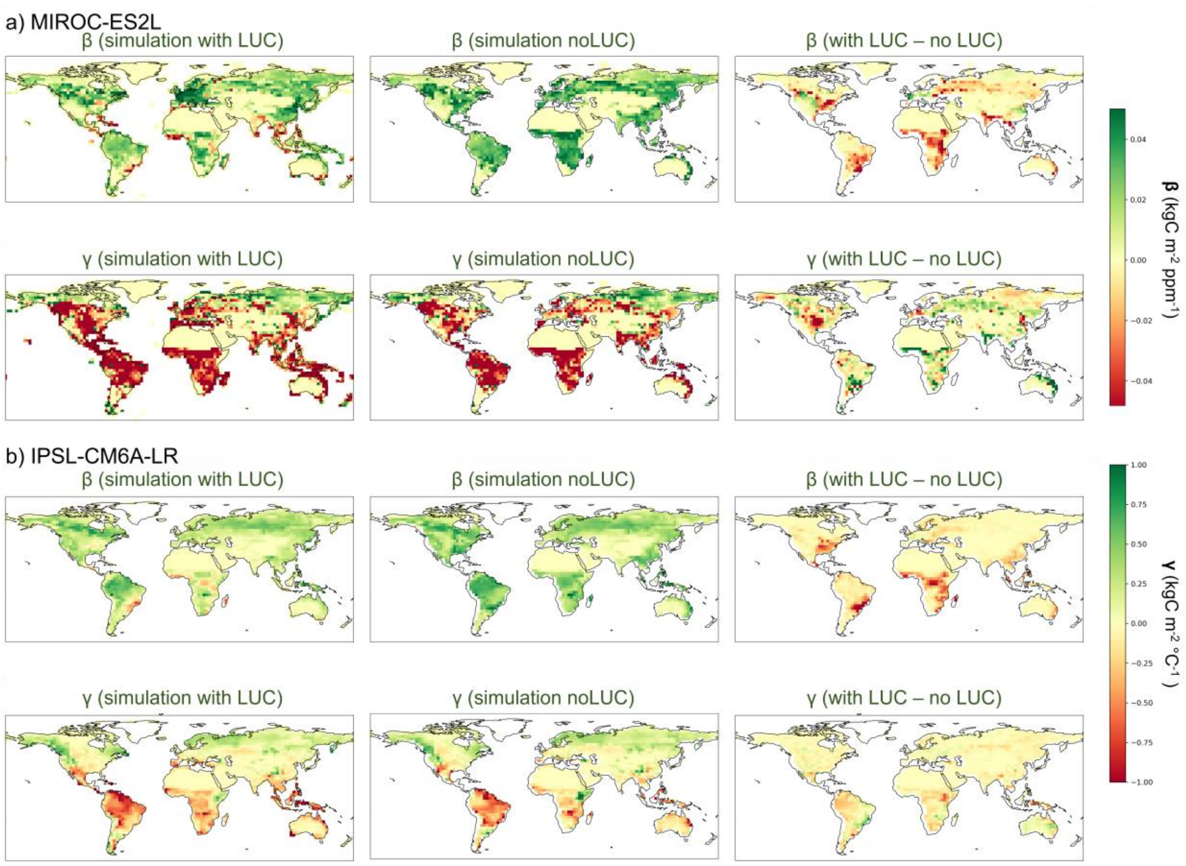

Figure S9: Spatial distributions of the of β and γ parameters by (a) MIROC-ES2L and (b) IPSL-CM6A-LR given as a 2090–2100 decadal means in simulations with and without LUC, and their difference. The negative values indicate less sink or more source from land to atmosphere.

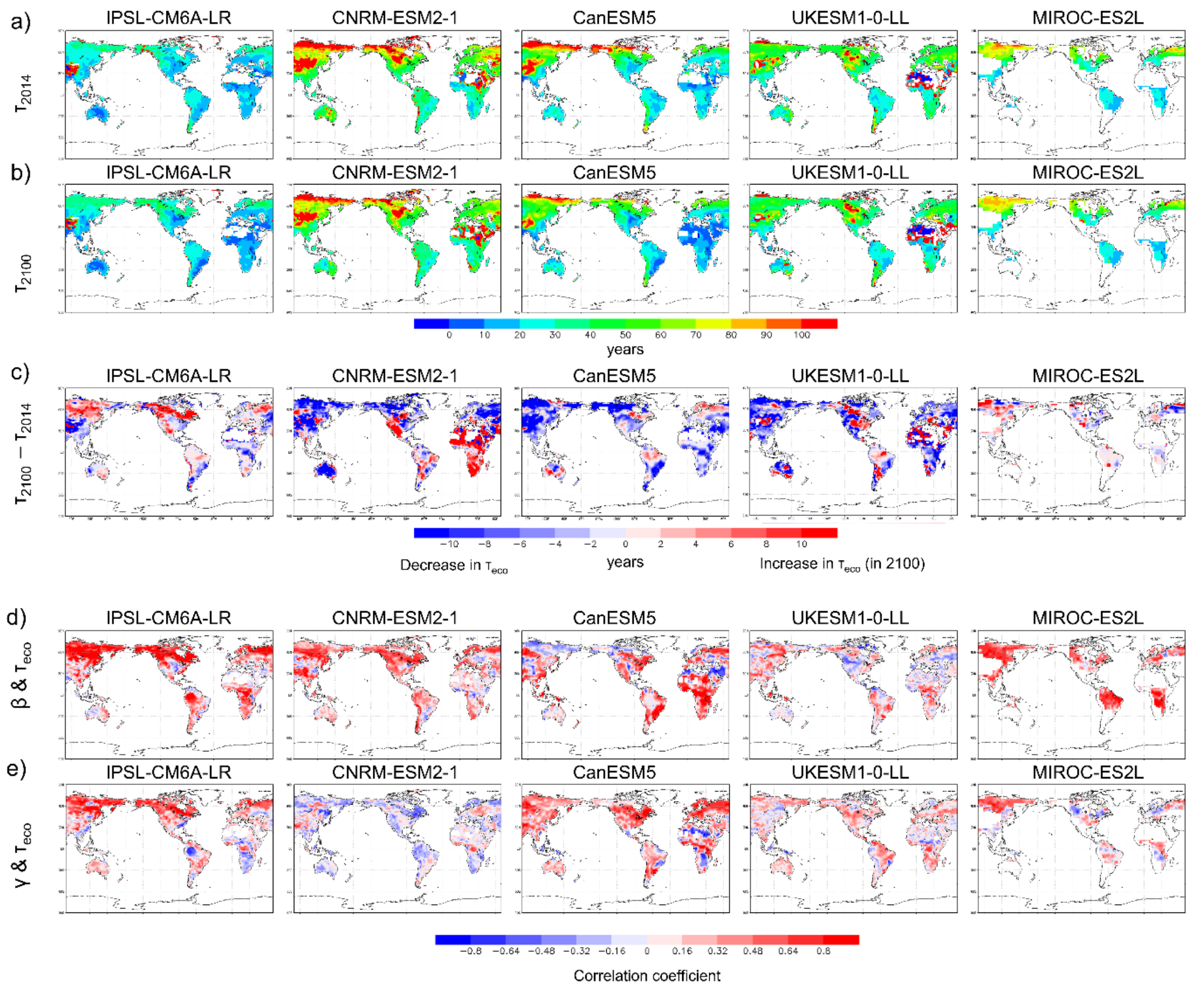

Figure S10: Spatial distributions of the carbon turnover time τ_{eco} in the years (a) 2014 and (b) 2100, and the difference in τ_{eco} between years 2100 and 2014 (the negative values indicate a decrease in τ_{eco} in 2100 from 2014 levels). The decrease in τ_{eco} indicates acceleration of carbon turnover. The correlation coefficients between τ_{eco} and (d) β and (e) γ feedback parameters that are estimated for the 2040 – 2100 period. The colormap is limited for MIROC-ES2L in the areas, where NPP is nearly zero and is also partly attributed to a relatively low spatial resolution of the model.